Analysis of radial-shear rolling process parameters of aluminum alloys based on FEM modeling

Yury Gamin[1*], *Alexander* Koshmin[1] and *Dinh Xuan* Ta[1]

[1]Department of Metal Forming, National University of Science and Technology "MISIS", 119049, 4 Leninskiy prospect, Moscow, Russia

Abstract. This article presents the features of temperature change at different deformation-velocity parameters of radial-shear rolling process. Based on modeling the maps of temperature and strain rates distribution and zone of intensive heating are obtained. It is shown that with the elongation ratio μ≥1.5, the deformation heating increases more intensively at lower heating temperatures of the workpiece. The rods are obtained from 1050A alloy (Al99.5 %) with mechanical properties (UTS ~ 111 MPa, YS ~ 109 MPa, δ ~ 15%), reflecting the partially recrystallized structure.

1 Introduction

Aluminum alloys are still one of the main constructional materials in aircraft industry, electrical engineering and other industries due to their combination of properties [1-3]. Modern trends of researchers' activities are connected, first of all, with the creation of new materials by change in chemical composition [4-6], improvement or search for new methods of processing materials [7-10]. In the field of materials science and metal forming in the last decades much attention is given to methods of severe plastic deformation (SPD) which allow significantly to increase the mechanical properties of the material due to ultra-fine grained (UFG) or nanostructures [11, 12]. At the same time, the main problem in application of SPD methods in industry is the inability to obtain semi-finished or large products. Thus, the urgent issue is development and studying of processing material methods which allow obtaining the product of acceptable sizes with high level of mechanical properties that are in demand in modern industry.

Radial-shear rolling (RSR) is one of methods for producing of long rods from different steels and alloys. [13-15]. Due to macro-shear deformation, the deep working of material structure takes place in deformation zone. [16-18]. Due to special calibration and large feed angle (β≥18°) the radial deformation (reduction) of workpiece takes place and the cross-sectional nonuniformity of deformation is reduced [19].

Formation of properties during deformation treatment depends on many factors, such as chemical composition of initial workpiece, temperature, strain rate and degree of

* Corresponding author: gamin910@gmail.com

© The Authors, published by EDP Sciences. This is an open access article distributed under the terms of the Creative Commons Attribution License 4.0 (http://creativecommons.org/licenses/by/4.0/).

deformation, deformation scheme, etc. Moreover, the influence degree of these parameters depending on alloy can vary greatly.

Based on the aforesaid the urgent scientific task is to study the characteristics of SRS process as method for obtaining semi-finished products from aluminum alloys To solve this task the combination of experimental study and FEM modeling is proposed [20-23], which makes possible to reduce the volume of laboratory experiments and study in detail the main parameters affected on formation of properties.

2 Experimental materials and Methods

Depending on deformation temperature it is possible to obtain the different combination of microstructures that will define mechanical properties of material. As it is known, many aluminum alloys have a tendency to intensive deformation heating. Heat effect at screw rolling is quite significant and depends on number of deformation cycle and value of reduction by each roll, for this reason in the study the analysis of temperature change is carried out at different elongation ratio and strain rates.

2.1 Experimental rolling

The cylindrical ingot with diameter of 60 mm from commercial-purity aluminum 1050A (Al99.5 %) was used as initial workpiece. The workpieces were rolled in 5 passes to a diameter of 14 mm with the total elongation ratio μ=18.4. Regimes of deformation are presented in table 1.

Table 1. Regimes of deformation.

Pass Number, i	Diameter of workpiece D_{i-1}, mm	Diameter of the resulting rod D_i, mm	Elongation ratio μ_i
1	60	42	2.04
2	42	31	1.84
3	31	24	1.67
4	24	17	1.99
5	17	14	1.47

The RSR mini-mill with work rolls with diameter of 90 mm which are turned by the feed angle of β=20° and toe angle δ=10° was used for rolling (Fig. 1).

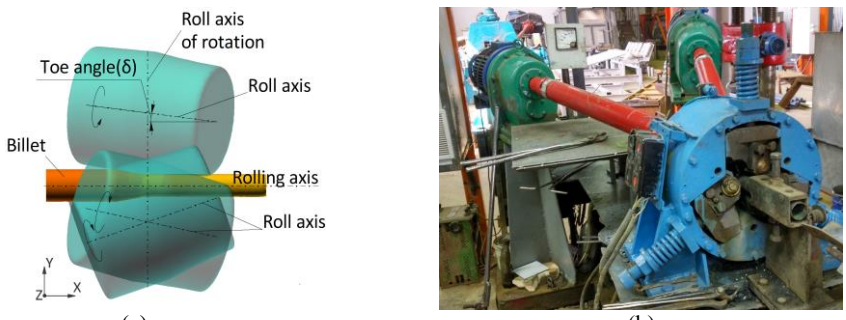

(a) (b)

Fig. 1. Principal scheme of RSR (a) and RSR mini-mill (b).

2

Before rolling, the workpieces were preheated to a temperature of T_0=200 °C and 250 °C. Rotary velocity of work rolls was set through the controlling system of main drive to 30 rpm.

As a result, two batches of rods at different temperatures were obtained. Room-temperature tension tests were conducted for as-processed bar specimens with a universal testing machine, model Zwick Z250 (the loading rate was 10 mm/min). According to test results the ultimate tensile stress (UTS), yield stress (YS) and elongation (δ) were obtained.

2.2 FEM simulation

Modeling of RSR process was carried out using software package QFORM 3D. To determine the dependences of temperature changes in the deformation zone during the RSR process, the workpieces were deformed at different elongation ratio μ=1.05; 1.1; 1.2; 1.6; 2.0; 2.4 (T_0=200 °C; n=30 rpm) and rotation velocity of work rolls n=10; 30; 60; 90 rpm (T_0=200 °C; μ=2.0). The main model parameters required for modeling are given in Table 2.

Table 2. Model parameters required for modeling of RSR process.

Parameter	Value
Toe angle δ (°)	10
Feed angle β (°)	20
Material of the roll	40Cr
Temperature of the roll (°C)	25
Ambient temperature (°C)	25
Coefficient of heat transfer between the material and the tool α (W/K·m^2)	30000
Coefficient of heat transfer between the material and the air α_{air} (W/K·m^2)	30

Temperature change of work tool and workpiece during deformation was calculated over total volume of contacted bodies in accordance with equation of transient heat conduction with account for heat transfer in environment on free surface:

$$q_n = b\alpha(T_1 - T_2), \quad (1)$$

where q_n - heat-transfer rate through heat transfer surface, W/m^2;
α – the heat transfer coefficient (W/K·m^2), which takes into account the complex of coefficients of heat transfer between workpiece and lubricant and between lubricant and tool;
T_1 - the workpiece temperature, K;
T_2 - the tool temperature, K;
$b=0.05$ – the pause coefficient which shows how many times it is necessary to reduce a heat transfer rate in the absence of tight contact between the workpiece and tool (without workpiece deformation).

3 Results and discussion

Based on modeling results the temperature distribution maps in the gorge in depending on different elongation ratio μ and velocity rotation of work rolls n were constructed (Fig. 2).

At small value of elongation ratio (μ=1.05-1.1) there is not deformation heating. In zones of contact with the rolls, the decrease in temperature is caused by a lower tool

temperature. Beginning with μ=1.2 the surface heating of the rod is observed, which increases with growing of radial reduction of rod.

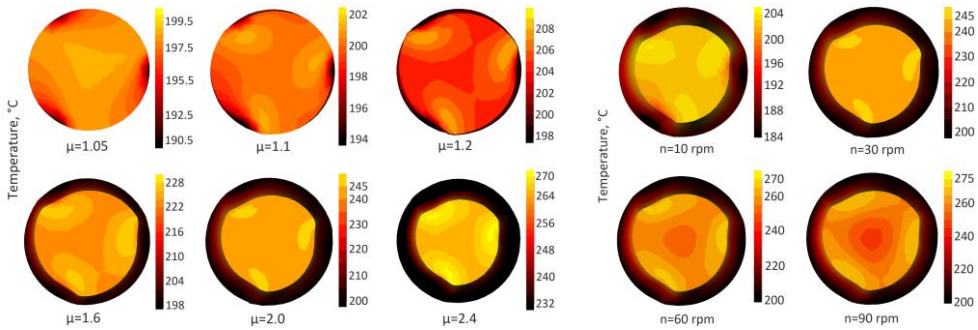

(a) (b)

Fig. 2. Temperature distribution maps over cross-section of rods (T_0=200 °C) at different elongation ration μ (a) and rotary velocity of work rolls n (b).

The most heating during RSR process can be observed in the near-surface layers of rod in contact zones with tool where deformation is located. This is also confirmed by the strain rate distribution maps over cross-section of the rod in the deformation zone (Fig. 3).

The change of temperature fields in depending on rotation velocity of work rolls is shown in Fig. 2 (b). With increasing in the rotation velocity of work rolls the temperature gradient also increases, which is due to more intensive heating of near-surface layers. At rotation velocity of 10 rpm the minimal temperature of rod is observed on surface of contact with tool, and total difference of temperatures is no more than 20 °C. At rotation velocity n=60 и 90 rpm the increasing in temperature of surface layer is grown to 70…75 °C, while temperature of center does not increase by more than 40 °C.

Determination of deformation zones and distribution nonuniformity of their influence can be observed by using values of strain rate (Fig. 3). In the deformation zone with increasing in reduction, the strain rate increases on the contact surfaces of rod with workpiece. Moreover, the values of strain rates in the central zone of workpiece do not practically change.

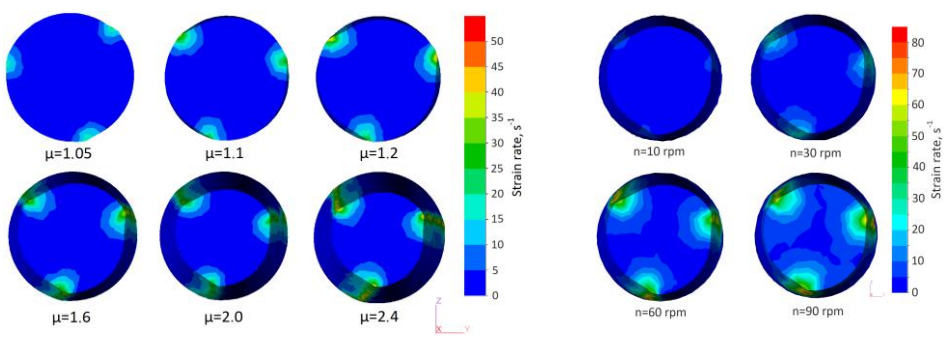

(a) (b)

Fig. 3. Strain rate distribution maps over cross-section of rods (T_0=200 °C) at different elongation ration μ (a) and rotary velocity of work rolls n (b).

The change in rotary velocity has significant effect on distribution of strain rates over cross-section of rod (Fig. 3, b). It can be observed that at rolling with rotary velocities n=60

and 90 rpm the strain rate in peripheral layer is an order of magnitude greater than in the center.

The formation processes of structure and properties by workhardening and dynamic recrystallization occurring during the deformation process are, first of all, associated with the deformation scheme, temperature and strain rate. The distribution data of these parameters which are obtained based on modeling, allow understanding the features of the zonal heterogeneity of the structure. For opportunity to evaluate obtained temperature distribution maps and to determine connection with formation of properties the graph of temperature changing ΔT at the exit of deformation zone as a function of reduction per pass was plotted (Fig. 4).

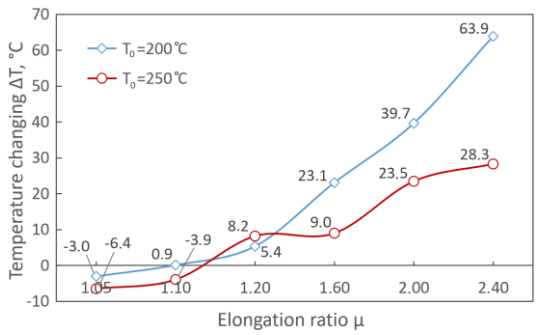

Fig. 4. The dependence of temperature changing ΔT on elongation ratio μ.

The temperature changing ΔT was calculated as difference between T_0 and average value of rod temperature at three points: in the center, middle of the radius, and near the surface. At small value of elongation ratio (μ≤1.2) the difference in temperature heating for rods heated to 200 and 250 °C is insignificant. The heat effect is almost completely compensated by heat exchange with work rolls. The increasing in elongation ratio of more than 1.2 leads to temperature growth after deformation, moreover the heating of workpiece at T_0=200 °C is greater than at T_0=250 °C. Since the recrystallization temperature for commercial-purity aluminum is 250 °C according to obtained data on temperature changing and strain rates after RSR process it is possible to assume that in near-surface layers where temperature heating exceed this value the recrystallized structure will be formed, and in the central zone the deformed ones will be developed. This assumption is corresponded with the results of measuring the mechanical properties of the obtained rods (Table 3).

Table 3. Mechanical properties of A1050 alloy after RSR.

Heating temperature T_0 [°C]	YS [MPa]	UTS [MPa]	δ [%]
200	110	115	1,0
250	109	111	15

In accordance with the selected rolling regimes (Table 1), the maximum elongation ratio per pass does not exceed 2. For workpieces heated to T_0=200 °C, the temperature increase is ~40 °C, which does not exceed the temperature of the onset of recrystallization. These rods have high strength and low ductility that corresponding to properties of work-hardened metal. Upon heating at 250 °C the deformation heating in the surface layers is higher than recrystallization temperature which is expressed in a significant increase in ductility (δ~15%). It should be noted that with an increase in ductility, there is practically no decrease in UTS and YS.

4 Conclusion

In the article the parameters analysis of radial-shear rolling of 1050A aluminum alloy is carried out. Based on the FEM modeling, it is shown that nonhomogeneous dynamic change in the temperature-deformation parameters in the deformation zone occurs during the RSR process.

During rolling of aluminum alloy the significant heat effect is observed, which caused by local zones of deformation and friction. The maps of temperature and strain rates distribution at different elongation ratio and rotation velocity were obtained. The comparison of the data on change of temperature and mechanical properties of rods rolled at different temperatures shows that with a certain elongation ratio, temperature and rates, it is possible to obtain a structure where the peripheral part of rod will be completely recrystallized and fine-grained while the axial zone will be deformed which determines the mechanical properties of the material.

The data on distribution of temperature-deformation parameters obtained on basis of FEM modeling make possible to understand the features of zonal heterogeneity of structure and to predict the properties of rods after rolling.

The research was supported by Russian Science Foundation (project No. 19-79-00054).

References

1. G.E. Totten, D.S. MacKenzie. *Handbook of aluminium. Vol. 1. Physical metallurgy and processes.* (N.Y., Marcel Dekker Inc., 2003)
2. L.F. Mondolfo. *Aluminum Alloys: Structure and Properties* (Butterworths: London, UK, 1976)
3. E.A. Starke Jr., J.T. Staley. Progress in Aerospace Sciences, **32**, pp. 131-172 (1996)
4. N. Belov, N. Korotkova, T. Akopyan, K. Tsydenov. Metals, **9**(12) (2019)
5. Akopyan T. K., Belov N. A., Naumova E. A., Letyagin N. V. Materials Letters, **245**, pp. 110-113 (2019)
6. C. Watanabe, R. Monzen, K. Tazaki. J. Mater, Sci. **43**: 813 (2008)
7. B. Romantsev, A. Goncharuk, A. Aleshchenko et al. Int. J. Adv. Manuf. Technol. **97**: 3223 (2018)
8. B.A. Romantsev, Y.V. Gamin, A.V. Goncharuk et al. Metallurgist, **61**: 217 (2017)
9. V.A. Sheremet'ev, A.A. Kudryashova, X.T. Dinh et al. Metallurgist, **63**: 51 (2019)
10. A.V. Zinov'ev, A.N. Koshmin, A.Y. Chasnikov. Metallurgist, **63**: 422 (2019)
11. I. Sabirov, N.A. Enikeev, M.Yu. Murashkin, R.Z. Valiev. Bulk Nanostructured Materials with Multifunctional Properties. (Springer, 2015)
12. R.Z. Valiev, A.P. Zhilyaev, T.G. Langdon. Bulk Nanostructured Materials: Fundamentals and Applications. (John Wiley & Sons, 2013)
13. S.P. Galkin, B.A. Romantsev, D.X. Ta, Y.V. Gamin. Chernye Metally, **4**, 20-27 (2018)
14. T.K. Akopyan, N.A. Belov, A.S. Aleshchenko et al. Mater. Sci. Eng. A, **746**, 134-144 (2019)
15. S. Dobatkin, S. Galkin, Y. Estrin et al. J. Alloys Compd. **774**, 969-979 (2019)
16. T.K. Akopyan, A.S. Aleshchenko, N.A. Belov et al. Phys. Metals Metallogr. **119**: 241 (2018)

6

17. B.V. Karpov, P.V. Patrin, S.P. Galkin et al. Metallurgist, **61**: 884 (2018)
18. A. Stefanik, A. Morel, S. Mroz, P. Szota. Arch. Metal. Mater., **60,** 2, 809–813 (2015).
19. A.V. Fomin, A.S. Aleshchenko, I.M. Maslenniko et al. Metallurgist, **63**: 477 (2019)
20. G.Y. Deng, Q. Zhu, K. Tieu et al. J. Mater. Process. Technol., **240**, 200–208 (2017)
21. Gontarz, A., Tomczak, J., Pater, Z., Bulzak, T. Materials, **12**, 2917 (2019).
22. Çakırcalı, M., Kılıçaslan, C., Güden, M. et al. Int. J. Adv. Manuf. Technol. **65**: 1273 (2013)

7